

X-Ray diffraction and spectroscopic studies of the light-induced metastable state of a ethylenediamine nitrosyl ruthenium complex

Masaki Kawano,^{ab} Ayako Ishikawa,^c Yoshiyuki Morioka,^c Hiroshi Tomizawa,^d Ei-ichi Miki^d and Yuji Ohashi^{*ab}

^a CREST, Japan Science and Technology Corporation, Kawaguchi City, Saitama Pref. 332-0012, Japan

^b Department of Chemistry and Materials Science, Tokyo Institute of Technology, Tokyo 152-8551, Japan. E-mail: yohashi@chem.titech.ac.jp

^c Department of Chemistry, Faculty of Science, Saitama University, Urawa 338-8570, Japan

^d Department of Chemistry, College of Science, Rikkyo University, Tokyo 171-8501, Japan

Received 10th February 2000, Accepted 22nd May 2000

Published on the Web 26th June 2000

Blue-laser irradiation of a single crystal of the chloride salt of a cationic complex, *trans*-[Ru(en)₂(H₂O)(NO)]³⁺ (en = ethylenediamine), yielded MS₁ (a metastable state of end-on type) which is remarkably stable (decay temperature $T_d = 267$ K) compared with MS₁ of sodium nitroprusside Na₂[Fe(CN)₅(NO)] (SNP). No MS₂ state (side-on type) was observed by X-ray diffraction and IR spectroscopy. Even with a low population of 8% of the metastable species, the structure was clearly determined by X-ray analysis. For the first time, we observed an elongation of the N–O bond by X-ray diffraction, corresponding to a frequency downshift of the $\nu(\text{NO})$ stretching vibration. The remarkably long lifetime of the metastable state of *trans*-[Ru(en)₂(H₂O)(NO)]³⁺ compared with that of SNP is explained by a stereochemical analysis using reaction cavity diagrams.

Introduction

The light-induced metastable states (MSs) of transition-metal nitrosyl complexes have attracted the great interest of scientists in the fields of chemistry, physics, and materials science because of the intriguing physical/optical properties and the potential candidates for functional materials in memory devices.^{1–9} Upon irradiation by blue light at low temperatures, a long-living metastable molecule is produced *via* the excited states in a crystal and reaches a photo-stationary state. The metastable state reversibly decays to the ground state (GS) upon thermal activation or irradiation by red light. A number of spectroscopic studies have been performed on the metastable states, but a crystallographic approach is relatively rare owing to experimental limitations although it can directly provide three-dimensional information on the geometry. Rüdinger *et al.* have reported the first crystallographic study by neutron diffraction on a metastable state of sodium nitroprusside Na₂[Fe(CN)₅(NO)] (SNP) is well known as a representative compound producing two metastable states, MS₁ and MS₂, by blue-light irradiation.^{10,11} For the first time, Coppens and co-workers have investigated the metastable states of SNP, and several transition-metal nitrosyl complexes by X-ray crystallography.^{12–17} They have proposed that the MS₁ and MS₂ of SNP should be linkage isomers having the end-on and side-on co-ordination geometries of the NO ligand toward Fe, respectively. Their proposal rationalized experimental results previously reported on SNP.

One of the present authors (Y. M.) and his co-workers have been studying spectroscopically ruthenium nitrosyl complexes ligated by a variety of ligands, *e.g.* ethylenediamine, quinolinate derivatives, oxalate anions, and halide ions, to prepare complexes with various electronic states.⁹ From the investigation of a series of complexes they have found several ruthenium nitrosyl complexes with significantly high decay temperatures above 260 K which are more stable than the MS of SNP ($T_d(\text{MS}_1) = 182$ K, $T_d(\text{MS}_2) = 150$ K) and produce not MS₂ but only MS₁ upon blue-laser irradiation.^{9,18} In this paper

we describe the spectroscopic features, magnetic properties, crystal structure, and stereochemical analysis of the remarkably long lived MS of a cationic complex, *trans*-[Ru(en)₂(H₂O)(NO)]Cl₃ ($T_d = 267$ K).

Experimental

General procedures and methods

trans-[Ru(en)₂(H₂O)(NO)]Cl₃ was prepared by the method described in ref. 19(a) and recrystallized by a layer-diffusion method from a HCl–ethanol solution.

A 441.6 nm line from a He–Cd laser, several lines from an argon ion laser, and a 632.8 nm line from a He–Ne laser were used to produce MSs for spectroscopic measurements. A 427.7 nm line from a solid-state blue laser was utilized for X-ray analysis and ESR experiments. A 430.0 nm line from an OPO (optical parametric oscillator) system equipped with a YAG laser was used for IR experiments. The formation of MSs was monitored by infrared spectroscopy. The $\nu(\text{NO})$ band of the MS is observed in the region from 1750 to 1800 cm^{–1}, while that of the GS is observed at 1914 (single crystal) or 1904 cm^{–1} (KBr pellet). From the intensity of a metastable state band the population change can be estimated relatively. To evaluate absolute values of the population of a MS, the decrease of the intensity of the ground state band was measured.

Spectroscopic measurements

Fourier-transform infrared spectra were recorded on a JASCO FT/IR-5300 instrument. A single crystal (3.00 × 2.00 × 0.16 mm; irradiated diameter 1 mm) and a sample dispersed in a KBr pellet were attached to the cold finger of a liquid N₂ cryostat (Oxford Instruments, DN1754) equipped with CaF₂ windows. Temperature was controlled within 0.1 K by a hand-made circuit. For absorption measurements at 77 K on a single crystal, a Xe-lamp light source and a spectrometer equipped with an ICCD (intensifier charge-couple device; Princeton Instruments, ICCD-576G/1) were used. Resonance Raman

measurements were carried out on a single crystal kept at 77 K. The 441.6 nm line from a He–Cd laser was used for excitation of a sample and for Raman scattering. To obtain spectra of the ground state at the same temperature, a 632.8 nm line from a He–Ne laser was used. Raman spectra were recorded by a triple polychromator (JASCO, TRS-501) equipped with a liquid N₂-cooled CCD detector (Princeton Instruments, LN/CCD-1100PB). ESR spectra were recorded at 77 K on a JEOL JES-RE2X spectrometer using a single crystal.

Magnetic susceptibility measurements

Variable-temperature magnetic susceptibilities of a single crystal (12 mg) were measured by using a Quantum Design MPMS SQUID susceptometer. The crystal wrapped with a sheet of aluminum foil suspended in a plastic straw inside the susceptometer's cavity was irradiated *via* a quartz fiber with a He–Cd laser (441.6 nm) at intensities of 30, 150, and 300 mW cm^{−2}. At 10, 30, and 100 K no change of susceptibility was observed, which indicates that Ru remains low spin on irradiation.

X-Ray crystallography

Sample preparation. All crystals were mounted on the tips of glass fibers with epoxy and cooled to low temperatures (≈ 103 K) controlled by a Rigaku cryostat system equipped with a N₂ generator. In order to produce the MS, a 427.7 nm line has been used with a power of 300 mW cm^{−2} for 1 h. The direction of the laser beam was normal to (−1 1 0) and the polarization was parallel to (1 1 0). Freshly prepared crystals were used in each data collection. Different crystals were used for the GS and MS structures.

Data collection and reduction. Data were collected on a Siemens SMART CCD X-ray diffraction system controlled by a Pentium-based PC running the SMART software package.²⁰ Graphite-monochromatized Mo–K α ($\lambda = 0.71073$ Å) radiation was used with a Rigaku rotating anode generator (50 kV, 200 mA).²¹ After a crystal had carefully been centered within the X-ray beam and avoided aligning the crystallographic axis along a ϕ axis, a series of 25 frames measured at 0.25° increments of ω were collected with four different ϕ (0, 90, 180, 270°) values at a 2θ value of -32° to calculate the preliminary matrix parameters. The intensities were collected with ω -scan technique ($\Delta\omega = 0.25^\circ$) within the limits $0 < 2\theta < 131^\circ$ ($\sin \theta_{\max}/\lambda = 1.28$ Å^{−1}). The data collection strategy was as follows: (a) four sets of 723 frames, 5 s per frame, detector arm at $\theta = -32^\circ$, $\phi = 0, 90, 180, 270^\circ$; (b) four sets of 723 frames, 5 s per frame, detector arm at $\theta = -55^\circ$, $\phi = 0, 90, 180, 270^\circ$; (c) four sets of 723 frames, 7 s per frame, detector arm at $\theta = -80^\circ$, $\phi = 0, 90, 180, 270^\circ$; (d) four sets of 723 frames, 10 s per frame, detector arm at $\theta = -102^\circ$, $\phi = 0, 90, 180, 270^\circ$.²² The initial 50 frames of the first data shell were recollected at the end of data collection to correct any overall crystal decay, but in each data collection no decay was observed.

After collection, the raw data frames were integrated by the SAINT program package.²³ The orientation matrix was updated every 40 frames during frame integration. After integration, the least-squares refinement was performed for the cell parameters using 8192 reflections from the first shell. Crystallographic details are summarized in Table 1.

Structure refinement. All structures were solved by use of the direct method program XS, part of SHELXTL, and refinements were carried out with SHELXL 97.²⁴ Anisotropic thermal parameters were applied to all non-hydrogen atoms unless noted. Scattering factors of the neutral atoms Ru, Cl, O, N, C, and H were taken from ref. 25. A single parameter was included to account for extinction effects.²⁶

Blue-laser irradiation with the wavelength of 430.0 nm

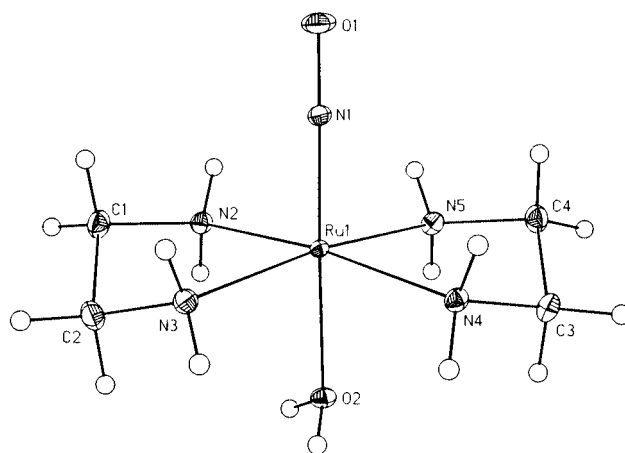


Fig. 1 Thermal ellipsoid (probability level 50%) plot of the ground state of *trans*-[Ru(en)₂(H₂O)(NO)]Cl₃ with the atom-labeling scheme.

excited a fraction of the ground state molecules to yield the MS in as much as 8% yield. Therefore, a small amount of the MS and a majority of the GS coexist in a crystal. The strategy to refine metastable and ground state molecules independently resulted in high correlations and no convergence. Application of rigid-group least-squares refinement to the GS avoided high correlations between metastable and ground state models. The anisotropic thermal parameters of the atoms of the ground state structure in the MS/GS refinement were fixed with those used in the refinement of the GS.

Empirical absorption corrections were calculated and applied for each structure with use of the SADABS program based on Blessings method.²⁷ Details of the least-squares refinement are summarized in Table 2.

CCDC reference number 186/1999.

See <http://www.rsc.org/suppdata/dt/b0/b001132k/> for crystallographic files in .cif format.

Results

Structure of the GS

Bond distances and angles of the cation are listed in Table 3 and a thermal ellipsoid plot of the structure is shown in Fig. 1. The geometry of the ground state structure is substantially in agreement with the earlier result,¹⁹ but is more accurate because of the lower temperature and the larger number of reflections with high redundancy collected for a whole sphere. Two difference maps (Fig. 2) in a section containing the Ru atom, the NO group, and the H₂O ligand, and in a section containing the Ru atom and four N atoms of ethylenediamine ligands, show the bonding features around the Ru atom, the NO group, and the H₂O ligand. With less reflections, the characteristic bonding features for the NO group were not clearly observed. Fig. 3 is a packing diagram of the ground state structure and the hydrogen-bonding network consisting of Ru–OH₂...Cl[−]...H₂NC₂H₄NH₂. The NO groups are aligned as a sheet along the *ab* plane but the NO direction alternates along the *c* axis.

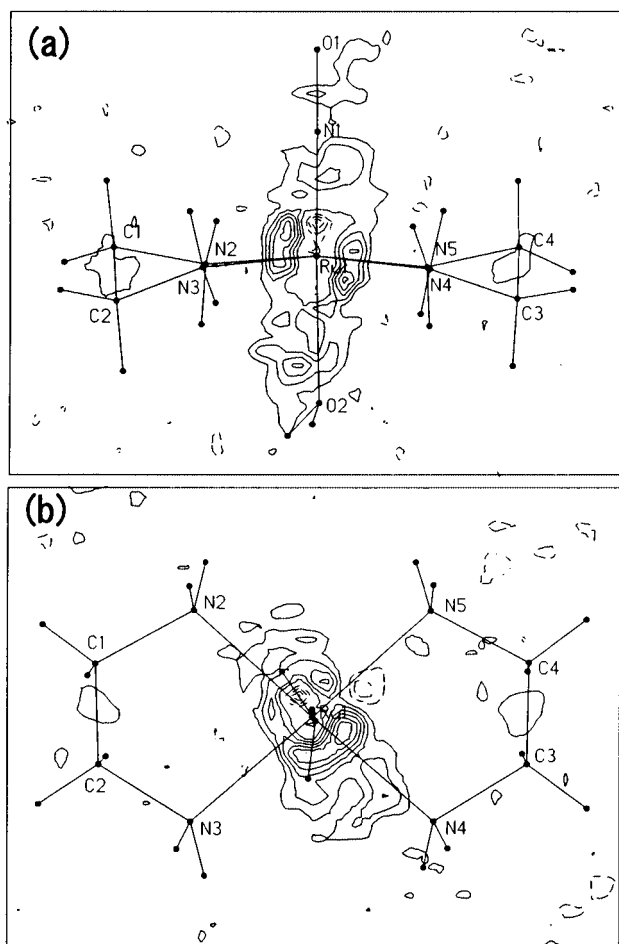
Structure of the MS

The first least-squares refinement for the chloride anions and the rigid group of the cation was performed to give final agreement factors of $R1 = 0.0237$, $wR2 = 0.0564$ and subsequent Fourier difference maps showed several new residual features ranging from 4.59 (0.32 Å from Ru1) to -1.41 (0.50 Å from Ru1) e Å³ (Fig. 4). Striking changes were found near the NO ligand and smaller changes near the ethylenediamine and H₂O ligands.

In the least-squares refinement procedure, the ground state structure was treated as a rigid group and isotropic thermal

Table 1 Experimental data for *trans*-[Ru(en)₂(H₂O)(NO)]Cl₃

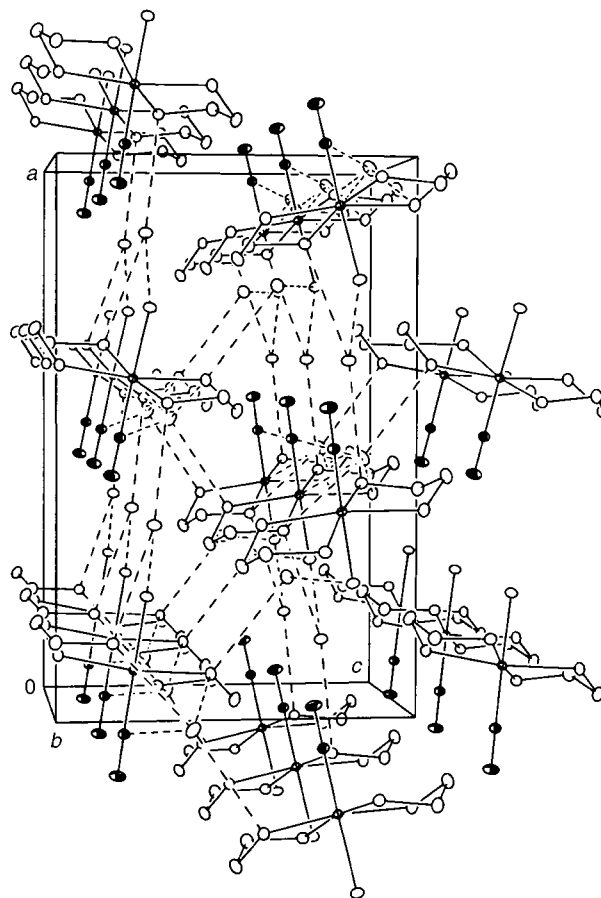
	GS	MS/GS ($\lambda_e = 427.7$ nm)
Crystal system, space group	Orthorhombic, <i>Pna</i> 2 ₁	
<i>T</i> /K	106	106
<i>a</i> /Å	15.4564(3)	15.4889(3)
<i>b</i> /Å	8.4266(2)	8.4263(2)
<i>c</i> /Å	10.0560(2)	10.0578(2)
<i>V</i> /Å ³	1309.75(7)	1312.68(7)
<i>Z</i>	4	4
μ /mm ⁻¹	1.80	1.80
No. reflections measured	141962	142280
No. symmetry unique reflections	22136	22032
Merging <i>R</i> (<i>I</i>), <i>R</i> (σ)	0.0286, 0.0192	0.0314, 0.0215
No. retained reflections with <i>I</i> > 2 σ (<i>I</i>)	20247	19518

**Fig. 2** Ground state residual map. The section contains (a) Ru1, the nitrosyl group, the water oxygen atom, and the centers of the ethylenediamine's C–C bonds and (b) Ru1 and the four nitrogen atoms of two ethylenediamine ligands (*ca.* 0.15 Å off out of the section). The contours are at 0.2 e Å⁻³, zero contour is omitted, and negative contours are indicated by broken lines.

parameters were applied to the MS. At first the occupancy factors of the GS and MS were fixed with values of 0.92 and 0.08, respectively, obtained from IR spectroscopy in order to avoid high correlations between the occupancy factors and the thermal and positional parameters. In the first attempt to refine a metastable state structure the Ru atom was divided into two, Ru1 and Ru1E, with occupancy factors of 0.92 and 0.08, respectively; Ru1E corresponds to the MS model. The refinement, however, led to a high correlation of 0.98 between the positional parameters of Ru1 and Ru1E, because Ru1E sits

Table 2 Summary of least-squares results

	GS	MS/GS ($\lambda_e = 427.7$ nm)	
		O-bound	N-bound
MS population	0	0.080(4)	0.077(5)
No. variables	209	86	86
<i>R</i> 1(<i>F</i>)	0.0152	0.0184	0.0184
<i>wR</i> 2(<i>F</i> ²)	0.0322	0.0375	0.0375
Goodness of fit	0.981	1.009	1.009
Flack <i>x</i> parameter	−0.004(6)	0.006(7)	0.006(7)
Highest residual peak, e Å ⁻³	1.51, −0.96	1.58, −1.74	1.59, −1.74

**Fig. 3** Packing diagram of the ground state *trans*-[Ru(en)₂(H₂O)(NO)]Cl₃.

very close to Ru1. Therefore, only one Ru atom with anisotropic thermal parameter free to refine in the ground state rigid group was applied to both the ground and metastable state models. The anisotropic thermal parameters of the other non-hydrogen atoms of the GS were fixed during refinement. This enabled an occupancy factor to be refined without a high correlation problem. All non-hydrogen atoms of the MS except that of the common Ru1 were refined with isotropic thermal factors.²⁸ The least-squares refinement of the occupancy factor of MS converged to 0.080(4) which is very close to a yield of 8.2% estimated by IR experiment using a 430 nm line from a YAG-OPO system instead of a 427.7 nm blue laser.

To clarify the possibility of a linkage isomer for MS, the two models of Ru–NO and Ru–ON were refined and the details are summarized in Table 2. Bond distances and angles in the cation are listed in Table 3. Plots with isotropic thermal vibration for comparison of Ru–NO with Ru–ON are shown in Fig. 5.

IR, UV-vis, and resonance raman spectroscopy

As shown in Fig. 6, the NO stretching frequencies of the GS

Table 3 Bond lengths [\AA] and angles [$^\circ$] for *trans*-[Ru(en)₂(H₂O)(NO)]Cl₃ (GS and MS) at 106 K

	GS	MS ($\lambda_e = 427.7$ nm)
Ru(1)–X ^a	1.7431(3)	1.834(4)
Ru(1)–O(2)	2.0592(3)	2.039(5)
Ru(1)–N(2)	2.1086(3)	2.116(4)
Ru(1)–N(3)	2.1170(3)	2.115(4)
Ru(1)–N(4)	2.1122(3)	2.129(4)
Ru(1)–N(5)	2.1022(3)	2.107(4)
N(1)–O(1)	1.1457(4)	1.169(6)
N(2)–C(1)	1.4930(6)	1.507(6)
N(3)–C(2)	1.4984(6)	1.499(7)
N(4)–C(3)	1.4983(5)	1.523(7)
N(5)–C(4)	1.4938(6)	1.496(7)
X–Ru(1)–O(2)	178.593(15)	178.49(17)
[O(1)–N(1)]Ru(1)	178.27(3)	177.8(3)

^a X = N in the GS; X = O in the MS.

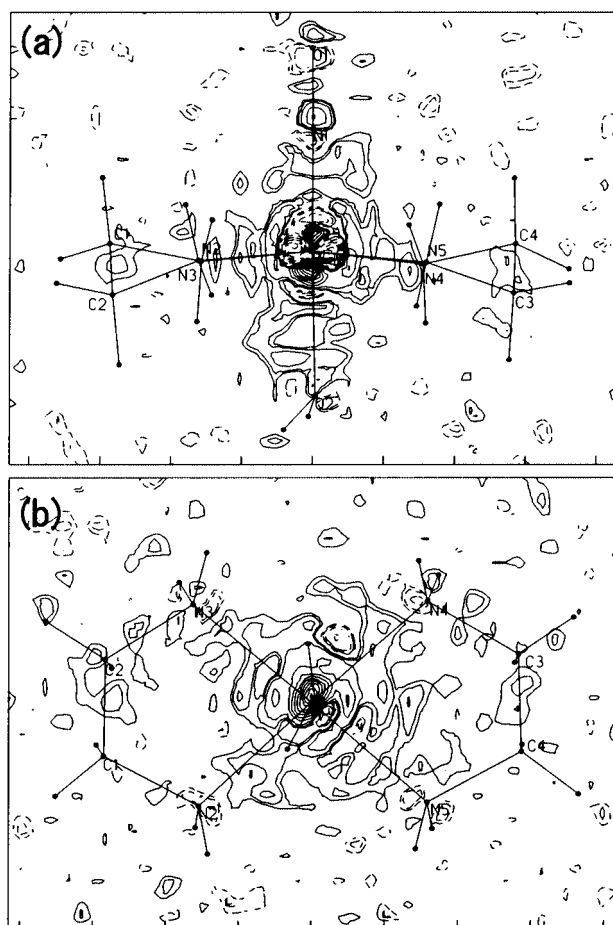


Fig. 4 MS – GS difference map (427.7 nm excitation). The section is as Fig. 2. Peaks, e \AA^{-3} (contour, e \AA^{-3}): (a) -4.77 to -0.5 (0.5), -0.3 , -0.2 , 0.2 , 0.2 , 0.3 , 0.5 to 4.23 (0.5); (b) -1.29 to -0.5 (0.5), -0.3 , -0.2 , 0.2 , 0.3 , 0.5 to 5.31 (0.5).

and MS of *trans*-[Ru(en)₂(H₂O)(NO)]Cl₃ in a single crystal occur at 1914 and 1773 cm^{-1} (1904 and 1786 cm^{-1} in a KBr pellet) and the second harmonics at 3779 and 3515 cm^{-1} , respectively. Fig. 6 and the IR spectra in a KBr pellet (not shown)⁹ suggest that blue-laser irradiation ($\lambda_e = 488.0$, 476.5, 457.9, 441.6 and 430.0 nm) at 77 K produced a single MS₁ species. No band corresponding to the MS₂ species was observed in the range from 1600 to 1650 cm^{-1} .²⁹

The absorption characteristic of M–NO adducts is weakly observed at 426 nm ($\epsilon = 17.8 \text{ M}^{-1} \text{ cm}^{-1}$) in a 6 M HCl solution of the GS.¹⁹ The small absorption coefficient makes possible light penetration throughout a single crystal. Blue laser (441.6

nm) excitation of a single crystal produced a broad absorption band in the region from 500 to 700 nm (Fig. 7). On the other hand, red laser (632.8 nm) excitation reproduced the ground state spectrum. Actually, the crystal slightly changed from yellow to brownish yellow on blue laser irradiation. This fact also indicates that blue laser irradiation of *trans*-[Ru(en)₂(H₂O)(NO)]Cl₃ yields no bluish MS₂ species like that observed for SNP.

The resonance Raman spectrum of the MS/GS of *trans*-[Ru(en)₂(H₂O)(NO)]Cl₃ is shown in Fig. 8. The electronic transition in which excitation takes place is assumed to be a metal (Ru)-to-ligand (NO) charge transfer. Obvious changes were observed at *ca.* 590 and 490 cm^{-1} assigned to the stretching or bending modes of Ru–NO. The spectroscopic feature is similar to that of the MS₁ of SNP.³⁰

Magnetic properties

The results of ESR and susceptibility measurements revealed that the ground state of *trans*-[Ru(en)₂(H₂O)(NO)]Cl₃ is diamagnetic with a low spin state. For the ESR measurements a single crystal was set up in a quartz tube and irradiated with blue lines (441.6 and 427.7 nm) at 77 K from the same direction as that used in the X-ray diffraction measurement. The ESR spectra were silent with/during excitation. In addition, the susceptibility measurements of the MS/GS induced with 441.6 nm excitation at 10 and 100 K gave a diamagnetic result. These facts indicate the MS remains low spin and the MS₁ is not a relaxed derivative induced by metal-to-ligand charge transfer from the highest occupied d_{xy} orbital to π^* of the NO orbital or to a d_z orbital, although initially a charge transfer model was proposed to explain the MS. Even Mössbauer spectroscopic³¹ and ESR³² studies of the metastable states of SNP show that they remain low spin on irradiation.

Discussion

Change of geometry

The bond distance of Ru–NO (1.7431(3) \AA) in the ground state structure is comparable to those of ethylenediamine nitrosyl ruthenium complexes with a nitrogen atom of ethylenediamine *trans* to a NO group.³³ The Ru–NO angle of 178.27(3) $^\circ$ is also in the typical range for ruthenium nitrosyl ethylenediamine complexes, indicating that those are of Ru^{II}–N⁺O type.

According to the Fourier difference map of Fig. 4, the Ru atom of the MS is slightly shifted from that of the GS toward the H₂O ligand and two ethylenediamine ligands of the MS are severely overlapped with those of the GS. Since the Ru atom in the rigid group of the GS was also used for the Ru atom of the MS model, bond distances and angles around Ru in the MS may have a considerable amount of error. Comparison of isotropic thermal parameters for Ru–NO and Ru–ON (Fig. 5) indicates that the light-induced metastable species is a linkage isomer as observed for SNP.¹⁵ If the Ru–NO model were used in 427.7 nm excitation, the isotropic thermal parameter of the oxygen atom was 20 times larger than that of the nitrogen atom. By contrast, the Ru–ON model led to a reasonable result. The bond distance of Ru–NO was drastically elongated by 0.091(4) \AA from 1.7431(3) \AA to 1.834(4) \AA on irradiation, which is identical with the Ru–NO bond distance change of 0.097(11) \AA (from 1.768(2) to 1.868(9) \AA) in K₂[Ru(NO)₂(OH)(NO)] (MS₁) at 50 K.¹⁴ In contrast, the Ru–NO angle of *trans*-[Ru(en)₂(H₂O)(NO)]Cl₃ remains linear but that of K₂[Ru(NO)₂(OH)(NO)] decreases from 174.0(2) to 169(1) $^\circ$.

Badger's rule^{10,34} predicts 0.026 \AA for the elongation of the NO bond expected from the frequency downshift by 118 cm^{-1} from 1904 to 1786 cm^{-1} (in a KBr pellet), which is in good agreement with the observed value of 0.023(6) \AA . The remarkable downshift of $\nu(\text{NO})$ and the elongation of the NO bond indicate that the contribution of π -back donation from

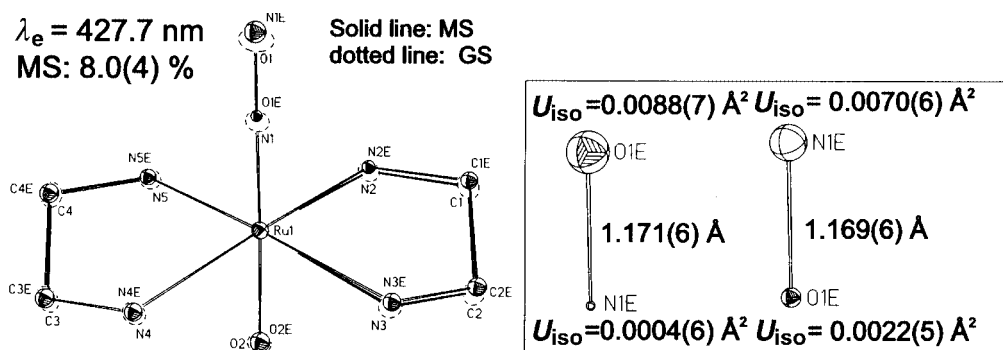


Fig. 5 Thermal ellipsoid plots for comparison of Ru–NO with Ru–ON.

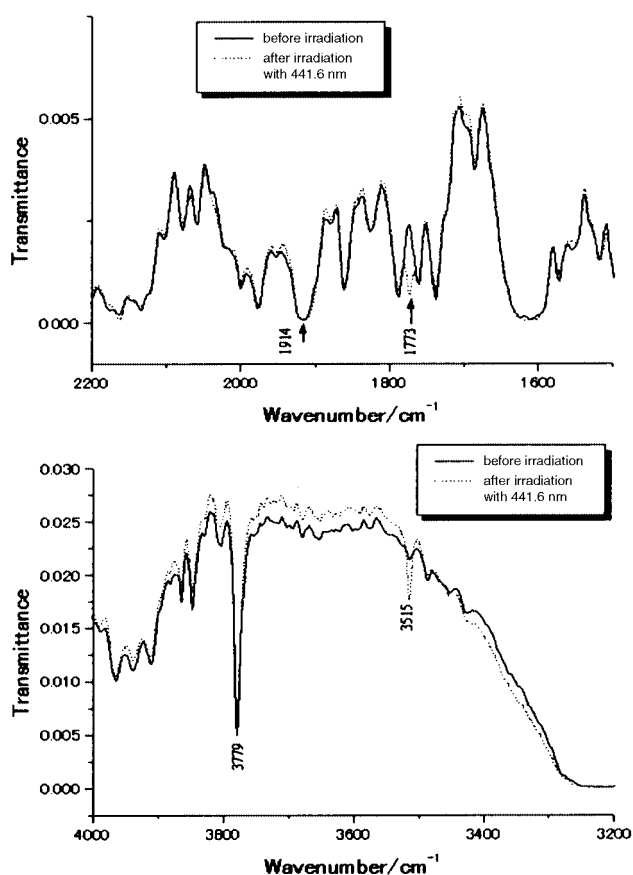


Fig. 6 IR spectra of the MS/GS in a single crystal at 77 K.

ruthenium to the NO ligand significantly increased in the MS.³⁵ If the Ru–NO structure were retained on irradiation, the Ru–NO bond length should decrease due to the increase of the π -back donation, but its significant elongation (0.091(4) Å) was observed. From this point of view, it is also reasonable that the light-induced metastable state should be a linkage isomer possessing the Ru–ON conformation.

Although, except for Ru–NO, significant changes (more than 3σ) of bond distances were observed in Ru–N4(en) (from 2.1122(3) to 2.129(4) Å by 0.017(4) Å) and N4–C3(en) (from 1.4983(5) to 1.523(7) Å by 0.025(7) Å), we have found no spectroscopic evidence and no chemically rational explanation for such changes. Ethylenediamine ligands so severely overlap each other in the GS/MS (with a low population) that it is generally difficult to refine both GS and MS models correctly. A theoretical calculation is necessary to verify the structural changes.

Spectroscopic features

Upon irradiation the downshift of the $\nu(\text{NO})$ stretching vibration by 118 cm^{-1} corresponds to those of transition-metal

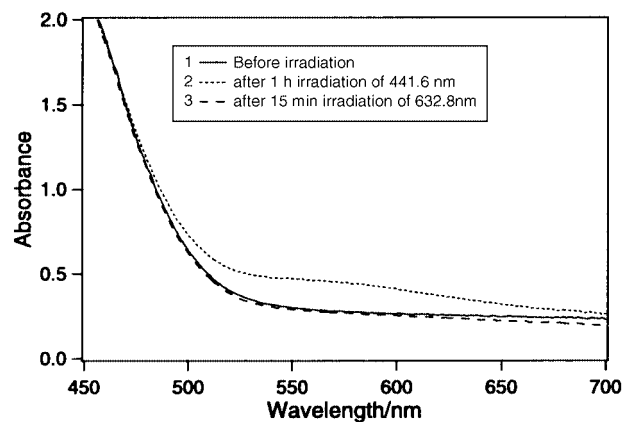


Fig. 7 Visible absorption spectra (GS-MS/GS) of *trans*-[Ru(en)₂-(H₂O)(NO)]Cl₃ at 77 K (sample: a single crystal of 281 μm thickness).

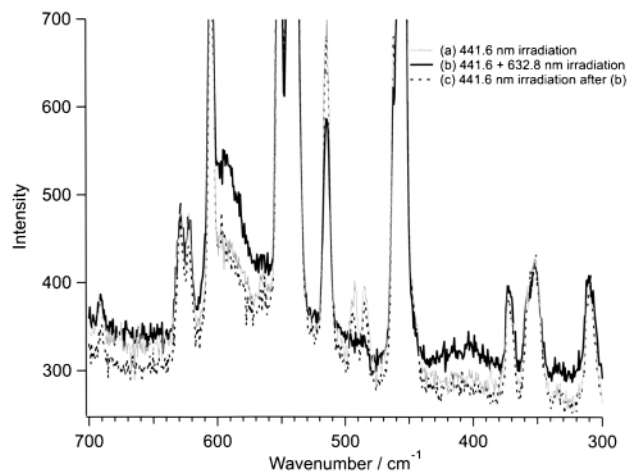


Fig. 8 Resonance Raman spectrum (RRS) of the MS/GS in a single crystal at 77 K. (a) RRS obtained by 441.6 nm irradiation. (b) RRS of GS obtained by 441.6 + 632.8 nm combined irradiation. (c) 441.6 nm irradiation performed after (b).

nitrosyl complexes such as SNP (113 cm^{-1})³¹ and $\text{K}_2[\text{Ru}(\text{NO}_2)_4(\text{OH})(\text{NO})]$ (114 cm^{-1}).²⁹ Although no clear changes of $\nu(\text{Ru–N})$ and $\delta(\text{Ru–N–O})$ in infrared spectra were observed owing to severe overlap of bands and small intensity changes, resonance Raman spectroscopy with 441.6 and 632.8 nm excitation enhanced spectral changes in the corresponding region. The ground state $\nu(\text{Ru–N})$ and $\delta(\text{Ru–N–O})$ are assigned to around 590 cm^{-1} corresponding to those of $\text{K}_2[\text{Ru}(\text{NO})\text{Cl}_5]$ ($604, 585 \text{ cm}^{-1}$).³⁶ As shown in Fig. 8, upon irradiation the intensity of the broad bands decreased and new bands emerged at 492 and 484 cm^{-1} , which are reasonably assigned to $\nu(\text{Ru–O})$ and $\delta(\text{Ru–O–N})$, respectively, as the case of a linkage isomer.

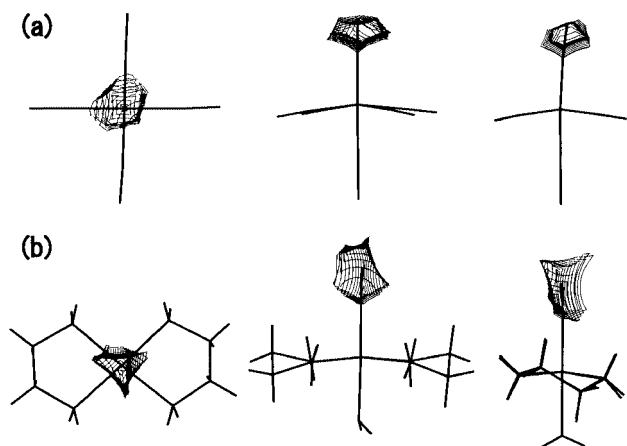


Fig. 9 Cavity diagrams (top, side 1 and side 2). (a) $[\text{Fe}(\text{CN})_5(\text{NO})]^{2-}$ (cavity size = 1.2 \AA^3), (b) $[\text{Ru}(\text{en})_2(\text{H}_2\text{O})(\text{NO})]^{3+}$ (cavity size = 1.3 \AA^3).

Stereochemical analysis

Not all transition-metal nitrosyl complexes produce a MS on irradiation. Chemical reactions depend upon both steric and electronic characteristics of the substrate. In sharp contrast to liquid reactions, a steric factor plays an important role in solid state reactions.³⁷ To estimate the steric repulsive force, the reaction cavities for the NO groups in SNP and *trans*- $[\text{Ru}(\text{en})_2(\text{H}_2\text{O})(\text{NO})]\text{Cl}_3$ were calculated and depicted in Fig. 9. The reaction cavity is defined as a concave limited by the envelope surface to the spheres, whose centers are positions of inter- and intra-molecular atoms in the neighborhood of the nitrosyl group, the radius of each sphere being greater by 1.2 \AA than the van der Waals radius of the corresponding atom. Obviously SNP has an ideal cavity suitable for side-on and end-on co-ordination, even for the disordered side-on geometry as described in ref. 15. On the other hand, *trans*- $[\text{Ru}(\text{en})_2(\text{H}_2\text{O})(\text{NO})]\text{Cl}_3$ has a narrow void tight for side-on co-ordination (see the first diagram of Fig. 9b; the wall has hollows) but large enough for the NO ligand to flip to form end-on co-ordination, Ru–ON (see the second and the third diagram of Fig. 9b). It seems reasonable that the ruthenium complex forms a remarkably long-lived MS compared with SNP.

Prior to our work, upon excitation the changes of N–O bond distances of transition-metal nitrosyl complexes determined by X-ray diffraction have been reported to be smaller than those expected from the frequency shifts of $\nu(\text{NO})$. This might be attributed to the mobility of the NO group. Larger mobility may make the observed N–O bond distance shorter.³⁸ In a system such as SNP that produces a MS_2 species of side-on type, the NO group has high mobility in a cavity. However, as with the MS_1 of SNP, the theoretical work by Delley *et al.* indicates that the N–O bond is not lengthened, even though the frequency is downshifted.³⁹ This needs to be clarified with further experimental/theoretical work.

Conclusion

We have investigated the spectroscopic and magnetic properties and the crystal structure of the light-induced metastable state of *trans*- $[\text{Ru}(\text{en})_2(\text{H}_2\text{O})(\text{NO})]\text{Cl}_3$. Even with a low population of 8% of the metastable species, the structure of the metastable state has been determined by X-ray analysis. For the first time, we have observed an elongation of the N–O bond by X-ray diffraction, in accordance with the downshift of the $\nu(\text{NO})$ stretching vibration. The remarkably long lifetime of the metastable state of *trans*- $[\text{Ru}(\text{en})_2(\text{H}_2\text{O})(\text{NO})]\text{Cl}_3$ compared with SNP is well explained by the reaction cavities for the NO groups in the crystals. Although the electronic factors play a crucial role in generation of metastable species from nitrosyl complexes upon excitation, a suitable steric environment is necessary.

Acknowledgements

This work was supported by CREST.

References

- U. Hauser, V. Oestreich and H. D. Rohrweck, *Z. Phys. A*, 1977, **280**, 17.
- T. Woike, W. Krasser, P. S. Bechthold and S. Haussühl, *Phys. Rev. Lett.*, 1984, **53**, 1767.
- H. Zöllner, W. Krasser, P. S. Bechthold and S. Haussühl, *Chem. Phys. Lett.*, 1989, **161**, 497.
- S. Haussühl, G. Schetter and T. Woike, *Opt. Commun.*, 1995, **114**, 219.
- J. A. Güida, P. J. Aymonino, O. E. Piro and E. E. Castellano, *Spectrochim. Acta, Part A*, 1993, **49**, 535.
- J. A. Güida, O. E. Piro and P. J. Aymonino, *Inorg. Chem.*, 1995, **34**, 4113.
- Y. Morioka, *Solid State Commun.*, 1992, **82**, 505.
- Y. Morioka, *Spectrochim. Acta, Part A*, 1994, **50**, 1499.
- K. Ookubo, Y. Morioka, H. Tomizawa and E. Miki, *J. Mol. Struct.*, 1996, **379**, 241.
- M. Rüdinger, J. Schefer, G. Chevrier, N. Furer, H. U. Güdel, S. Haussühl, G. Heger, P. Schweiss, T. Vogt, T. Woike and H. Zöllner, *Z. Phys. B*, 1991, **83**, 125.
- M. Rüdinger, J. Schefer, T. Vogt, T. Woike, S. Haussühl and H. Zöllner, *Physica B*, 1992, **180** and **181**, 293.
- M. R. Pressprich, M. A. White and P. Coppens, *J. Am. Chem. Soc.*, 1993, **115**, 6444.
- M. R. Pressprich, M. A. White, Y. Vekhter and P. Coppens, *J. Am. Chem. Soc.*, 1994, **116**, 5233.
- D. V. Fomitchev and P. Coppens, *Inorg. Chem.*, 1996, **35**, 7021.
- M. D. Carducci, M. R. Pressprich and P. Coppens, *J. Am. Chem. Soc.*, 1997, **119**, 2669.
- P. Coppens, D. V. Fomitchev, M. D. Carducci and K. Culp, *J. Chem. Soc., Dalton Trans.*, 1998, **6**, 865.
- D. V. Fomitchev, T. R. Furlani and P. Coppens, *Inorg. Chem.*, 1998, **37**, 1519.
- Y. Morioka, A. Ishikawa, H. Tomizawa and E. Miki, *J. Chem. Soc., Dalton Trans.*, 2000, **5**, 781.
- H. Tomizawa, E. Miki, K. Mizumachi and T. Ishimori, (a) *Bull. Chem. Soc. Jpn.*, 1994, **67**, 1809; (b) *Bull. Chem. Soc. Jpn.*, 1994, **67**, 1816.
- SMART, Version 4.0, Siemens Industrial Automation, Inc., Madison, WI, 1995.
- A CCD area detector has been found well suited for electron density studies on a reference crystal of an angiotensin II receptor antagonist, and the $\lambda/2$ contamination, which affects area detectors but not well tuned conventional detectors, proves to be a negligible source of errors (P. Macchi, D. M. Proserpio, A. Sironi, R. Soave and R. Destro, *J. Appl. Crystallogr.*, 1998, **31**, 583). $\lambda/2$ contamination is much more of a problem for small hard inorganic crystals than macromolecules. With the rotating anode setting used in our study it would be expected it to be evident in these data sets, though its effects will still be minor (K. Kirschbaum, A. Martin and A. A. Pinkerton, *J. Appl. Crystallogr.*, 1997, **30**, 514).
- This strategy provided 99.4% coverage in $\sin(\theta/\lambda) < 1.28 \text{ \AA}^{-1}$ and high redundancy of data which is especially important for the SADABS program to work efficiently.
- SAINT, Version 5.0, Siemens Industrial Automation, Inc., Madison, WI, 1998.
- SHELXL 97, Crystal Structure Analysis Program, UNIX version, G. M. Sheldrick, 1993–1997, Release 97-2.
- International Tables for Crystallography*, ed. A. J. C. Wilson, Kluwer Academic Publishers, Dordrecht, 1992, vol. C, Tables 6.1.1.1 (pp. 500–502), 4.2.6.8 (pp. 219–222), and 4.2.4.2 (pp. 193–199).
- A. C. Larson, *Crystallographic Computing*, eds. F. R. Ahmed, S. R. Hall and C. P. Huber, Munksgaard, Copenhagen, 1970, pp. 291–294.
- R. H. Blessing, *Acta Crystallogr., Sect. A*, 1995, **51**, 33.
- The positional change of the Ru atom before/after modeling the metastable state is as follows. Before modeling (right after the initial Fourier difference calculation): Ru1 0.107931 0.280042 0.303673. After the refinement including the metastable model: Ru1 0.107954 0.280017 0.303671. This indicates that the Ru atom position shifted by less than 0.001 \AA after the refinement. Likewise the N1 position of a nitrosyl group in the rigid group shifted by less than 0.001 \AA .
- e.g., $\text{K}_2[\text{Ru}(\text{NO}_2)_4(\text{OH})(\text{NO})]$, $\nu_{\text{MS}_2}(\text{NO})$ 1623 cm^{-1} ; $\text{Na}_2[\text{Fe}(\text{CN})_5(\text{NO})] \cdot 2\text{H}_2\text{O}$, $\nu_{\text{MS}_2}(\text{NO})$ 1665 cm^{-1} .
- For SNP, $\delta_{\text{GS}}(\text{Fe–N–O})$ (E) 669 cm^{-1} , $\nu_{\text{GS}}(\text{Fe–N})$ (A_1) 662 cm^{-1} ; $\delta_{\text{MS}_1}(\text{Fe–N–O})$ (E) 582 cm^{-1} , $\nu_{\text{MS}_1}(\text{Fe–N})$ (A_1) 565 cm^{-1} , based on the

- results of polarized Raman spectroscopic studies using a ^{15}N isotope (Y. Morioka, S. Takeda, H. Tomizawa and M. Ei-ichi, *Chem. Phys. Lett.*, 1998, **292**, 625); GS vibrations, L. Tosi, *Spectrochim. Acta, Part A*, 1973, **29**, 353; J. B. Bates and R. K. Khanna, *Inorg. Chem.*, 1970, **9**, 1376; MS vibrations based on Raman scattering measurement, W. Krasser, Th. Woike, S. Haussühl, J. Kuhl and A. Breitschwerdt, *J. Raman Spectrosc.*, 1986, **17**, 83; MS vibrations based on polarized IR absorption measurement, J. A. Güida, P. J. Aymonino, O. E. Piro and E. E. Castellano, *Spectrochim. Acta, Part A*, 1993, **59**, 535.
- 31 U. Hauser, V. Oestreich and H. D. Rohrweck, *Z. Phys. A*, 1977, **280**, 125; Th. Woike, W. Kirchner, H. Kim, S. Haussühl, V. Rusanov, V. Angelov, S. Ormandjiev, Ts. Bonchev and A. N. F. Schroeder, *Hyperfine Interact.*, 1993, **7**, 265.
 - 32 C. Terrile, O. R. Nascimento, I. J. Moraes, E. E. Castellano, O. E. Piro, J. A. Güida and P. J. Aymonino, *Solid State Commun.* 1990, **73**, 481.
 - 33 Ru–NO bond distances: 1.757(7) Å in *cis*-[RuCl(en)₂(NO)]Cl[PF₆], 1.751(8) Å in *cis*-[Ru(NCS)(en)₂(NO)]I₂·H₂O, ref. 19(b) 1.727(6) (X = Cl), 1.738(5) (X = Br), 1.736(15) Å (X = I) in [RuX₃(en)(NO)], H. Tomizawa, K. Harada, E. Miki, K. Mizumachi, T. Ishimori, A. Urushiyama and M. Nakahara, *Bull. Chem. Soc. Jpn.*, 1993, **66**, 1658.
 - 34 D. R. Hershbach and V. W. Laurie, *J. Solid State Phys.*, 1961, **35**, 458.
 - 35 Another possible reason for the lowering of frequency for $\nu(\text{NO})$ can be a rehybridization of the lone pair at O on co-ordination. To elucidate the electronic state of the MS, theoretical calculation will be necessary.
 - 36 M. J. Cleare, H. P. Fritz and W. P. Griffith, *Spectrochim. Acta, Part A*, 1972, **28**, 2013.
 - 37 Y. Ohashi, K. Yanagi, T. Kurihara, Y. Sasada and Y. Ohgo, *J. Am. Chem. Soc.*, 1981, **103**, 5805; Y. Ohashi, A. Uchida, Y. Sasada and Y. Ohgo, *Acta Crystallogr., Sect. B*, 1983, **39**, 54; Y. Ohashi, *Acc. Chem. Res.*, 1988, **21**, 268; K. Sawada, D. Hashizume, A. Sekine, H. Uekusa, K. Kato, Y. Ohashi, K. Kakinuma and Y. Ohgo, *Acta Crystallogr., Sect. B*, 1996, **52**, 303.
 - 38 J. Dunitz, *X-Ray Analysis and the Structure of Organic Molecules*, VCH, New York, 1995, p. 248.
 - 39 B. Delley, J. Schefer and Th. Woike, *J. Chem. Phys.*, 1997, **107**(32), 10067.